

SPIN-POLARIZED PROPERTIES OF Ni-DOPED ZnSe: FIRST-PRINCIPLES SIMULATION AND MODELLING

 V.N. Jafarova^{a,b,*},  A.N. Jafarova^a,  A.J. Ahmadova^c

^aAzerbaijan State Oil and Industry University, 20 Azalig Ave., AZ-1010, Baku, Azerbaijan

^bKhazar University, 41 Mehseti Str., AZ1096, Baku, Azerbaijan

^cNakhchivan State University, AZ-7012, Nakhchivan, Azerbaijan

*Corresponding Author E-mail: vusala.cafarova@asoiu.edu.az

Received June 1, 2025; revised August 8, 2025; accepted August 19, 2025

This work delivers an in-depth *ab initio* investigation into the electronic and magnetic characteristics of ZnSe systems doped with nickel, evaluated at three distinct impurity levels: 3.125%, 6.25% and 12.5%. The analysis is grounded in density functional theory (DFT), employing the local spin density approximation (LSDA) framework, further refined with Hubbard U corrections to effectively capture the pronounced electron correlation effects typical of transition metal d-electrons. The incorporation of Ni into the ZnSe matrix significantly modifies the electronic structure, leading to half-metallic behavior and pronounced spin polarization. Total magnetic moments of 4.0 μ_B per supercell were observed. Furthermore, energy comparisons between ferromagnetic and antiferromagnetic configurations confirmed that the ferromagnetic phase is more energetically stable. These results highlight the potential of Ni-doped ZnSe in spintronic applications where controlled magnetic and electronic properties are crucial.

Keywords: ZnSe:Ni; Ferromagnetic; Half-metal; Magnetic moment; First-principles simulation; Density Functional Theory

PACS: 61.72.-y; 75.50.Pp; 68.55.Ln

1. INTRODUCTION

Diluted Magnetic Semiconductor materials (DMSMs) have significantly advanced systems science by facilitating the development of multifunctional compounds that exhibit a combination of magnetic behavior and semiconducting capabilities. These hybrid functionalities make DMSs particularly attractive for next-generation applications in engineering, environmental monitoring, optoelectronics, and especially in the rapidly developing field of spintronics, where control over electron spin is essential.

Compared to other potential diluted magnetic semiconductor (DMS) hosts, ZnSe offers several key advantages that make it a particularly promising candidate for spintronic applications. For instance, ZnO, despite being widely studied, suffers from the formation of intrinsic defects such as oxygen vacancies and zinc interstitials, which lead to unintentional n-type conductivity and hinder the achievement of stable p-type behavior [1]. CdTe and ZnTe, while possessing favorable electronic characteristics, exhibit stronger spin-orbit coupling and involve cadmium—a toxic element that raises serious environmental and safety concerns [2]. ZnS, moreover, demonstrates limited solubility for transition metal (TM) dopants and lacks consistent experimental confirmation of room temperature ferromagnetism [3].

In contrast, ZnSe presents a well-balanced and advantageous profile. It combines a favorable wide direct band gap (Exp.: ~2.7 eV [4]; 2.763 eV [5]) with relatively low spin-orbit coupling enhancing spin coherence and facilitating spin transport in devices [6], [7] along with excellent chemical and thermal stability. Its structural compatibility with standard thin-film growth techniques further enables efficient dopant incorporation and device fabrication [3]. These combined characteristics make ZnSe an attractive host matrix for TM-doped DMS systems aimed at spin-based applications.

Studying the electronic and magnetic properties of ZnSe doped with transition metals such as Ni is essential for evaluating its potential as a functional DMS. The material's electronic structure dictates critical device-relevant properties, optical response, electrical conductivity, and carrier mobility, while TM-induced magnetic behavior is key to achieving room-temperature ferromagnetism vital for spintronic operations. Of particular interest is half-metallicity, where one spin channel is metallic and the other semiconducting, enabling fully spin-polarized currents at the Fermi level. Such characteristics are fundamental to devices like spin valves, magnetic tunnel junctions, and spin field-effect transistors.

This focus aligns with established theoretical and experimental advancements in DMS physics. Dietl et al. [8] developed a seminal mean-field model of hole-mediated ferromagnetism in tetrahedrally coordinated semiconductors, which underpins much of DMS theory development. Tanaka and Higo demonstrated large tunneling magnetoresistance in GaMnAs/AlAs/GaMnAs junctions, highlighting the functionality of ferromagnetic semiconductors in device contexts [9]. Foundational also are visionary perspectives on spintronics and DMSs provided by Wolf et al. [10] and Awschalom & Flatté [11], as well as first-principles formulations by Sato et al., which collectively guide and justify material selection and device design strategies [12].

Moreover, the role of intrinsic defects is critical in DMS performance. Defects such as vacancies and interstitials can dramatically influence magnetic coupling including mechanisms like bound magnetic polaron formation and may either stabilize or inhibit ferromagnetic ordering. Importantly, defect-dopant interactions can be harnessed to tailor band

gaps, control charge carrier density, and enhance magneto-optical effects. Understanding this interplay is therefore essential for optimizing ZnSe-based DMS materials.

This work aims to provide a comprehensive first-principles investigation into the electronic structure, magnetic behavior, and defect effects in Ni-doped ZnSe supercells. By comparing undoped and doped configurations and analyzing spin-resolved band structures and densities of states, we identify the origins of half-metallicity and spin polarization in $\text{Zn}_{1-x}\text{Ni}_x\text{Se}$. These results contribute to the fundamental understanding of II–VI DMS systems and support the future design of spin-based optoelectronic devices.

Zinc selenide (ZnSe), a II–VI compound semiconductor, is inherently non-magnetic and possesses a direct band gap of approximately 2.70 eV [4], which makes it highly suitable for various optoelectronic devices. Its applications span from laser diodes, lasers, and light-emitting diodes to solar cells, microwave and terahertz emitters, and mid-infrared (IR) tunable lasers [11–13]. However, by introducing transition metal (TM) dopants such as Co or Ni into the ZnSe lattice, its properties can be significantly tailored to exhibit spin polarization and ferromagnetic behavior - transforming the material into a DMS.

Numerous studies have focused on TM-doped $\text{Zn}_{1-x}\text{TM}_x\text{Se}$ compounds, recognizing their potential as functional materials for spin-based electronic and magnetic devices [14–21]. For example, Sato et al. [12, 22] predicted high Curie temperatures in Cr- and V-doped ZnSe using first-principles simulations based on a zinc-blende structure. Similarly, theoretical investigations by Benstaali et al. [15] on Co-doped ZnSe, Mahmood et al. [23] on Ti-doped ZnSe, and Arif et al. [24] on Co-doped CdSe revealed half-metallic ferromagnetic phases, confirming the viability of these materials for spintronic technologies.

Our earlier work [25] demonstrated that the introduction of a Zn vacancy in Mn-doped ZnSe leads to half-metallic ferromagnetism, supporting the idea that defects and dopants together play a critical role in tuning the magnetic characteristics of such systems. In the present study, we extend this line of investigation to Ni-doped ZnSe with one and two doping concentrations: 3.125 %, 6.25% and 12.5%. Using first-principles DFT simulations, we analyze the electronic structure, spin polarization, and magnetic ordering (ferromagnetic vs. antiferromagnetic) of the doped systems. Our findings reveal that the incorporation of Ni ions induces robust ferromagnetic ordering and high spin polarization, transforming ZnSe into a ferromagnetic semiconductor. This highlights its potential application in spintronic devices where efficient spin injection and manipulation are required.

The primary novelty of this work lies in the systematic first-principles study of the electronic and magnetic properties of Ni-doped ZnSe, specifically at doping concentrations of 3.125 %, 6.25% and 12.5%. By applying spin-polarized density functional theory (DFT), we analyze the impact of nickel doping on the electronic structure, magnetic ordering, and half-metallicity of ZnSe. This work offers new insights into the fundamental behavior of diluted magnetic semiconductors (DMS), particularly in how transition metal doping can tune the material's properties to make them suitable for spintronic applications.

The purpose of this study is to explore how Ni doping influences the magnetic and electronic properties of ZnSe, focusing on the emergence of half-metallic ferromagnetism and spin-polarization in the material. In doing so, we investigate the role of nickel in modifying the band structure and inducing a spin asymmetry, which is critical for future spintronic devices such as spin valves and magnetic tunnel junctions.

The motivation behind this work is rooted in the growing demand for materials that can simultaneously exhibit semiconducting and magnetic properties, crucial for advancing spin-based technologies. While previous studies have investigated other DMS systems, our work emphasizes ZnSe as an ideal candidate due to its favorable electronic characteristics and minimal spin-orbit coupling. Our findings contribute to expanding the understanding of Ni-doped ZnSe, offering a pathway for designing new materials for applications in spintronics, where controlling electron spin is essential for efficient device operation.

In light of these considerations, this manuscript presents an in-depth study with a clearly defined objective, ensuring that the research not only contributes to the scientific community but also addresses the challenges in developing high-performance DMS materials for next-generation technologies.

2. CALCULATION METHOD

In this research, *ab initio* simulations were carried out within the framework of DFT, coupled with the pseudopotential method [26] for analyzing the electronic and magnetic characteristics of semiconductors, half-metals, and nanoscale materials. The computational framework was implemented using the Atomistix ToolKit (ATK, <http://quantumwise.com/>) integrated within the Virtual NanoLab (VNL) simulation environment. The ATK was chosen for DFT calculations due to its integrated real-space basis and efficient treatment of spin-polarized systems in large supercells. ATK has been widely used in semiconductor studies for over a decade. Its reliability is supported by strong agreement with both experimental data and results obtained from other well-established DFT packages, confirming its suitability for modeling TM-doped ZnSe systems. Moreover, the calculations were completed within a relatively short PC time, demonstrating the software's computational efficiency for large-scale supercell models.

In our study, we also continuously explored various DFT-based methods, including LDA, GGA, MGGA, and hybrid functionals, to investigate the electronic and magnetic properties of the materials. Our experience showed that LDA and GGA, when combined with Hubbard U corrections, were successfully applied in the calculations. For most of

our calculations, we successfully used LDA and LSDA methods to model the electronic and magnetic properties. It should be noted that we also tested hybrid functionals for various compositions, but due to the considerably longer computational time required for these calculations, we decided to discontinue their use for the current study. The many-body interactions between electrons and atomic nuclei were treated within the Kohn-Sham formalism [27], which transforms the complex many-electron problem into a set of self-consistent one-electron equations. To solve these equations, we applied the linear combination of atomic orbitals method. The exchange-correlation effects were treated within the local spin density approximation, supplemented by Hubbard U corrections [28] to better account for the on-site Coulomb interactions, particularly for the localized d-electrons of the transition metals as reported in Refs. [29, 30]. In this study, the magnetism of diluted magnetic semiconductor systems $\text{Zn}_{1-x}\text{TM}_x\text{Se}$ was investigated under conditions similar to those used in previous works [25, 29, 30]. Supercell models were developed by replacing one or two Zn atoms with Ni^{2+} ions to simulate doping concentrations. Hubbard U corrections were applied to improve the accuracy of band gap predictions and to account for strong electron correlation effects associated with Ni 3d orbitals. In our calculations, the Hubbard U parameters were set as follows: Zn (3d) = 4.5 eV and Se (4p) = 3.8 eV.

To investigate the magnetic properties of Ni-doped ZnSe, supercell models consisting of 32 and 64 atoms were constructed based on the wurtzite ZnSe structure with initial lattice parameters $a = 3.98 \text{ \AA}$ and $c = 6.53 \text{ \AA}$, as reported in Refs. [31, 32]. Nickel doping was simulated by substituting one or two Zn atoms with Ni^{2+} ions, corresponding to doping concentrations of 3.125 %, 6.25% and 12.5%, respectively. Ni atoms were substituted at Zn sites in the ZnSe lattice, as the substitution is energetically favorable and commonly reported in the literature for DMS studies. Although Ni has a slightly smaller atomic radius ($\sim 1.24 \text{ \AA}$) than Zn ($\sim 1.34 \text{ \AA}$) [33], structural relaxation during DFT optimization showed no significant lattice distortion or clustering at the doping levels considered.

The crystal structure of ZnSe was assumed to be hexagonal, belonging to the $P6_3mc$ space group [29]. The electronic structure and spin-resolved properties were computed using norm-conserving pseudopotentials from the Fritz-Haber-Institute (FHI), along with a double-zeta polarized (DZP) basis set. The Brillouin zone integration was carried out using a $5 \times 5 \times 5$ Monkhorst-Pack k-point grid. The plane-wave energy cutoff was set to 100 Ry to ensure convergence of total energy and magnetic properties. In the Ni-doped ZnSe systems, the separation between Ni atoms depends on the size of the supercell. For the 32-atom supercell, the optimized Ni-Ni distance is 7.96 \AA , while in the 64-atom supercell, it increases to 9.50 \AA . This distance corresponds to the spatial separation between the two Ni dopant atoms along the [001] crystallographic direction (i.e., parallel to the c-axis of the supercell).

To illustrate this configuration, a representative figure is included below, showing the dopant positions and the direction along which the measurement was performed. During geometry optimization, both atomic positions and lattice vectors were fully relaxed. Structural relaxation was performed until the forces on each atom were below 0.001 eV/ \AA and the total stress was less than 0.001 eV/ \AA^3 . These settings ensure that the calculated Ni-Ni distances accurately reflect the relaxed equilibrium geometry in the ferromagnetic (FM) state of the system.

To analyze the distribution of magnetic moments, Mulliken population analysis was used. The calculations allowed for a detailed investigation of the magnetic ordering, spin polarization, and stability of different magnetic phases. Both ferromagnetic (FM) and antiferromagnetic (AFM) configurations were considered by appropriately arranging the spins of the Ni atoms ($\text{Ni}\uparrow\text{Ni}\uparrow$ and $\text{Ni}\uparrow\text{Ni}\downarrow$ configurations).

This computational approach provides a reliable basis for predicting the spin-polarized behavior of Ni-doped ZnSe:Ni at various doping levels and for assessing its potential use in spintronics.

3. RESULTS AND DISCUSSION

Electronic properties of ZnSe and ZnSe:Ni

Initially, the electronic band structures and density of states (DOS) for undoped ZnSe were calculated using supercells containing 32 and 64 atoms. In order to accurately determine the band gap and the dispersion relations of the bands, first-principles calculations were performed within the local spin density approximation (LSDA) framework, incorporating Hubbard U corrections for the Zn *d*- (4.5 eV) and O *p*-electrons (3.8 eV). To observe the changes induced in the electronic band structure upon Ni doping and for comparison purposes, the band structure of undoped ZnSe with a 32-atom supercell is presented in Figure 1.

It is worth noting that the band structure and band gap of the 64-atom ZnSe supercell are analogous. The calculated band gap of 2.70 eV for undoped ZnSe in this study is in good agreement with previous experimental results. For instance, wavelength-modulated spectroscopy reported a band gap of 2.70 eV [4], while other experimental studies have investigated the optical band gap properties of ZnSe and yielded a slightly higher value of 2.763 eV [5]. Additionally, optically-pumped lasing has been demonstrated in doped ZnSe epitaxial layers grown by metal-organic vapour-phase epitaxy [5].

Figure 2 illustrates the total density of states (TDOS) for undoped ZnSe using the 32-atom supercell. Based on the results of the band structure and DOS calculations for ZnSe, the valence band can be primarily divided into three distinct groups. The first group, located at the top of the valence band, mainly originates from the *p*-states of Se atoms. The second group of valence states is predominantly contributed by the *d*-orbitals of Zn atoms. The lowest-lying states (third group) are primarily derived from the *s*-states of Se atoms. As seen in Figures 1 and 2, the zones corresponding to spin-up and spin-down states in the band structure completely overlap, and the DOS curves are perfectly symmetric.

These results obtained for the electronic properties (electronic structure and DOS) indicate that the undoped ZnSe compound is a nonmagnetic material.

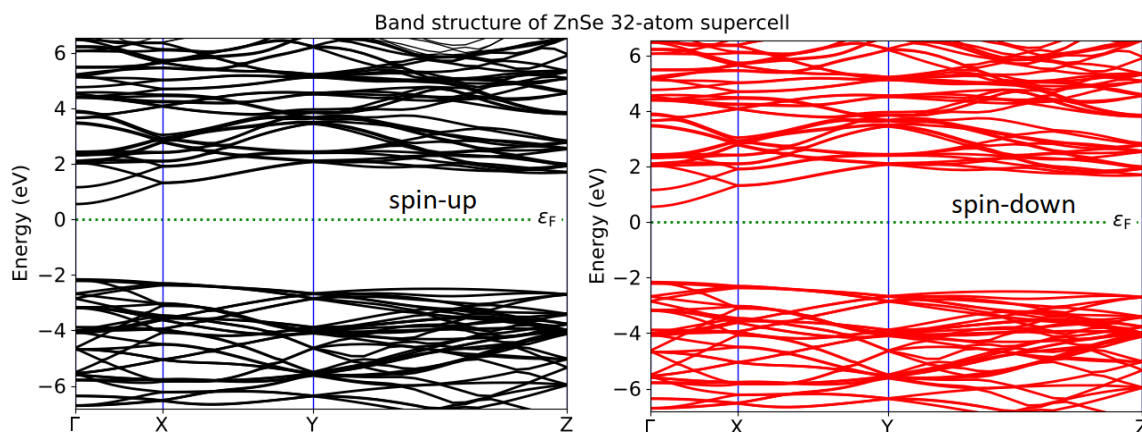


Figure 1. Spin-polarized band structure of undoped ZnSe supercell containing 32 atoms, calculated using first-principles methods

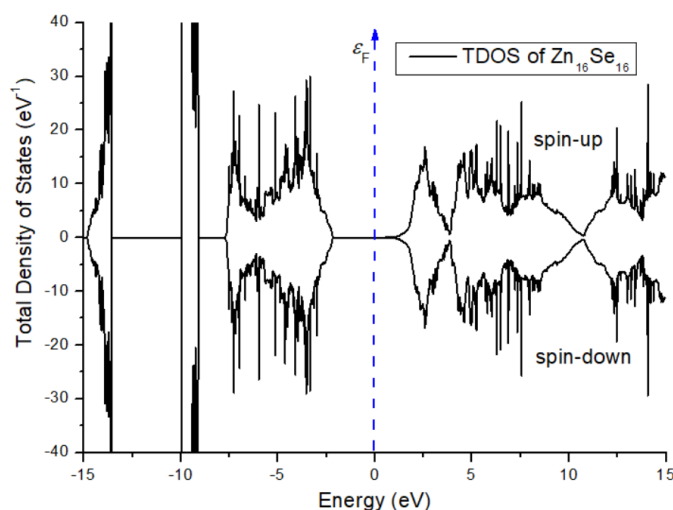


Figure 2. Spin-polarized TDOS diagram for undoped ZnSe supercell containing 32 atoms

The band structure interpretation of ZnSe:Ni supercells reveals that the incorporation of Ni atoms substantially modifies the band structure of the host semiconductor. Specifically, impurity-induced states emerge near the Fermi level, with some of these states crossing the Fermi energy. This behavior is a clear indicator of the onset of magnetic ordering in the system, driven by the interaction between the localized d-electrons of Ni and the host lattice. The calculated spin-polarized band structures for majority- and minority-spin channels, along with Figures 3 and 4 illustrate the total density of states (TDOS), while Figure 5 presents the partial density of states (PDOS) for Se and Ni atoms in the 32-atom Ni-doped ZnSe supercell.

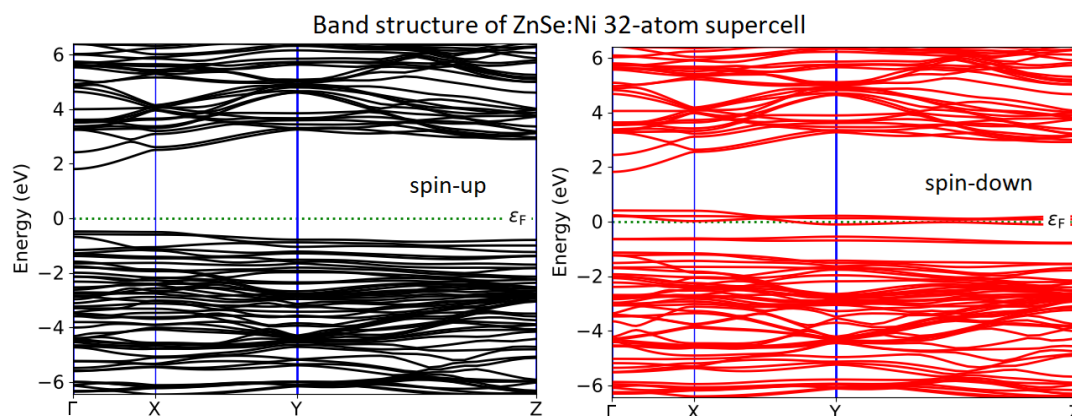


Figure 3. Spin-polarized band structure of Ni-doped ZnSe supercell containing 32 atoms, calculated using first-principles methods

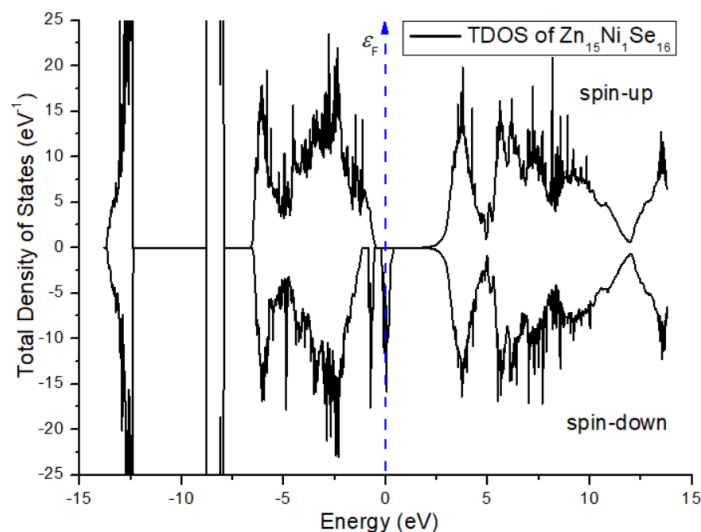


Figure 4. Spin-polarized TDOS diagram for a Ni-ZnSe supercell containing 32 atoms

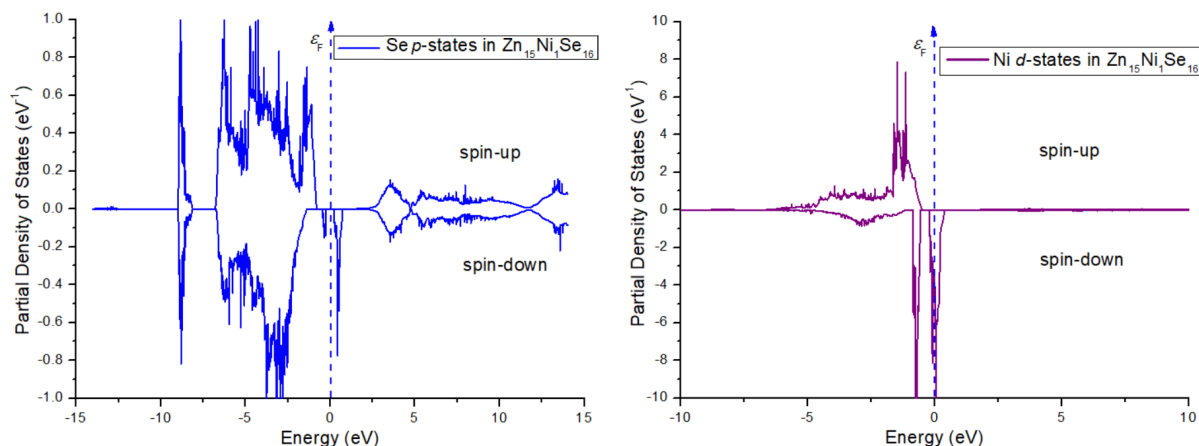


Figure 5. Spin-polarized PDOS diagram for Ni and Se atoms in Ni-ZnSe 32-atom supercell.

Additionally, from first-principles calculations, we have studied the electronic properties of a ZnSe 64-atom supercell doped with a Ni atom. The obtained band structures (minority and majority spin) and DOS curves are shown in Figures 6-8. The PDOS plot shows that Ni 3d orbitals contribute significantly to the DOS vicinity of Fermi energy. A significant hybridization occurs between the Ni 3d orbitals and the Se 4p states, most prominently in the spin-down state. This orbital mixing alters the band structure by introducing spin-dependent energy levels, which manifest as a distinct spin asymmetry in the DOS. The spin-up states exhibit a clear band gap, characteristic of semiconducting behavior, whereas the spin-down states retain metallic states at the Fermi level. Such properties are of particular interest for spintronic applications, where the control of spin currents is essential for device performance. The magnetic moment primarily originates from Ni 3d orbitals, while Se atoms also contribute slightly through p-d hybridization.

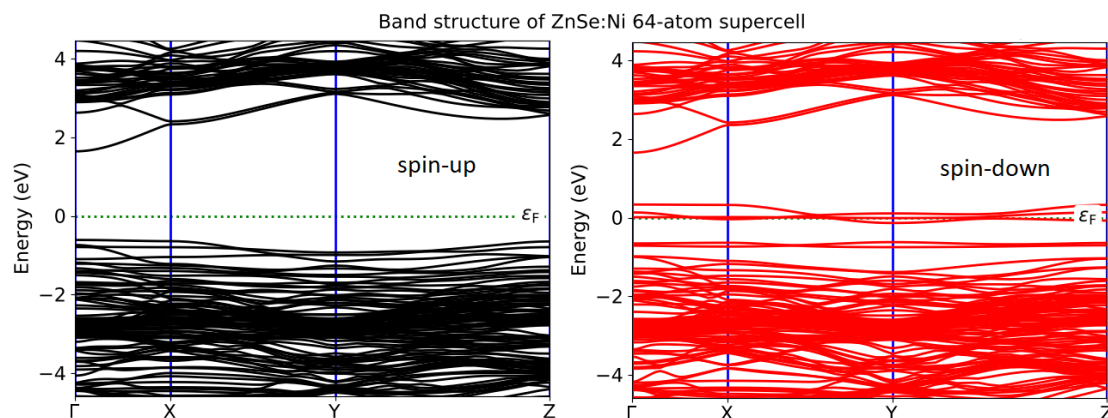


Figure 6. Spin-polarized band structure of Ni-doped ZnSe supercell containing 64 atoms, calculated using first-principles methods.

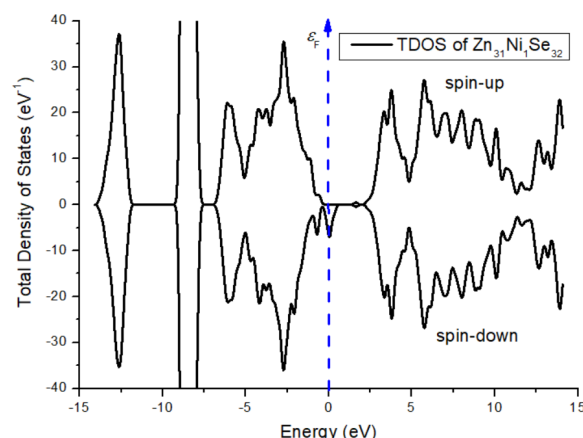


Figure 7. Spin-polarized TDOS diagram for a Ni-ZnSe supercell containing 64 atoms.

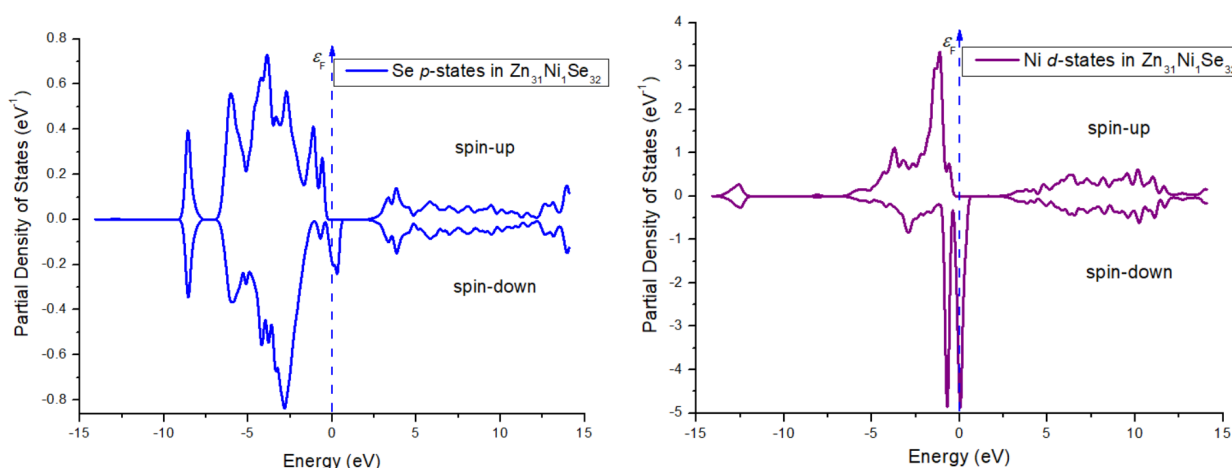


Figure 8. Spin-polarized PDOS diagram for Ni and Se atoms in Ni-ZnSe 64-atom supercell.

These findings emphasize the role of transition metal dopants and host atom interactions in tailoring the spintronic properties of ZnSe-based diluted magnetic semiconductors. A pronounced imbalance between the spin-up and spin-down electronic states is observed, providing clear evidence of spin polarization in the Ni-ZnSe system. This asymmetry indicates that the electronic structure favors one spin orientation over the other, a critical feature for materials considered in spintronic device design, where spin-selective transport plays a key role. The PDOS diagrams, shown in Figures 5 and 8, highlights strong hybridization between the Ni 3d orbitals and the Se 4p orbitals, which plays a crucial role in mediating the magnetic interactions. The replacement of Zn atoms with Ni introduces significant changes to the electronic structure, most notably causing a reduction in the band gap of the spin-up channel and inducing metallic behavior in the spin-down channel.

Table 1 presents the calculated band gap energies for both undoped and Ni-doped ZnSe supercells. For the undoped systems ($\text{Zn}_{16}\text{Se}_{16}$ and $\text{Zn}_{32}\text{Se}_{32}$), the band gaps are identical for both spin-up and spin-down channels (2.70 eV), indicating a symmetric electronic structure and confirming the non-magnetic nature of pure ZnSe. Upon Ni doping, significant spin polarization emerges. In the $\text{Zn}_{15}\text{Ni}_1\text{Se}_{16}$ supercell (6.25% Ni), the spin-up band gap decreases to 2.48 eV, while the spin-down band gap closes completely (0.00 eV), indicating the onset of half-metallic behavior. A similar trend is observed in the $\text{Zn}_{31}\text{Ni}_1\text{Se}_{32}$ supercell (3.125% Ni), where the spin-up gap further reduces to 2.24 eV, with the spin-down channel remaining metallic (0.00 eV). This spin-selective behavior, semiconducting in the spin-up channel and metallic in the spin-down, is a defining feature of half-metallic ferromagnetism. It is observed in both 32- and 64-atom ZnSe supercells doped with Ni, confirming that Ni incorporation introduces strong spin asymmetry and transforms the electronic structure of ZnSe.

Table 1. Band gap results for undoped and doped ZnSe

Supercells	x , %	Spin-up, eV	Spin-down, eV
$\text{Zn}_{16}\text{Se}_{16}$	0.0	2.70	2.70
$\text{Zn}_{32}\text{Se}_{32}$	0.0	2.70	2.70
$\text{Zn}_{15}\text{Ni}_1\text{Se}_{16}$	6.25	2.48	0.00
$\text{Zn}_{31}\text{Ni}_1\text{Se}_{32}$	3.125	2.24	0.00

Such half-metallic properties, characterized by a fully spin-polarized density of states at the Fermi level, are highly desirable for spintronic applications, as they enable efficient spin injection and control in advanced electronic and optoelectronic devices. These findings establish $\text{Zn}_{1-x}\text{Ni}_x\text{Se}$ as a promising candidate for next-generation spin-based technologies.

Ferromagnetic properties of ZnSe:Ni

The magnetic properties of $\text{Zn}_{1-x}\text{Ni}_x\text{Se}$ systems were analyzed using the Mulliken population method. Both the total and local magnetic moments were calculated for Ni-doped ZnSe systems, including the Ni^{2+} ions and their neighboring atoms. While pure ZnSe exhibits no magnetic behavior, doping with Ni ions induces magnetic properties in the system. The majority of the magnetization arises from the hybridization between the p-electronic states of the host selenium atoms and the d states of the Ni impurity ions.

Figure 9 presents the spin-polarization structure of the $\text{Zn}_{15}\text{NiSe}_{16}$ supercell from first-principles simulations. The black arrows indicate the magnetic moments of atoms: the lengths of these arrows are scaled according to the values of the corresponding magnetic moments.

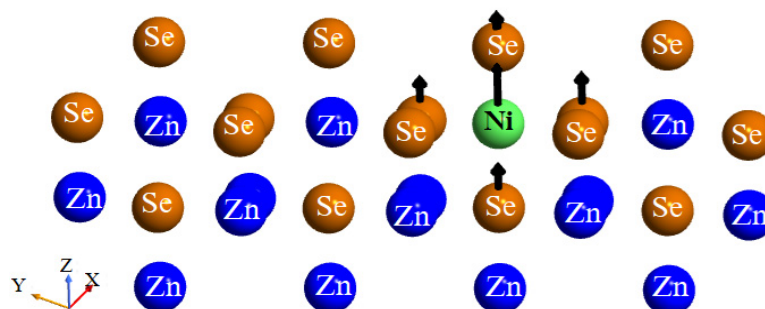


Figure 9. Spin-polarization map of the Ni-doped ZnSe 32-atom supercell.

For the Ni-ZnSe systems, the computed total magnetic moment within the examined supercell configurations is around $4 \mu_B$ per Ni dopant atom. Additionally, the local magnetic moment, primarily originating from the Ni site, contributes significantly to the overall magnetic behavior of the system, which localized specifically on each Ni ion is estimated to be about $1.2 \mu_B$. The dominant contribution to the overall magnetization primarily arises from the nickel ion's 3d electronic states, which provide nearly $1.2 \mu_B$ of magnetic moment. In contrast, the surrounding zinc atoms contribute only a negligible amount to the total magnetic moment, indicating that their role in the magnetic behavior of the system is minimal. Interestingly, a significant positive contribution to the magnetic moment also comes from four selenium atoms that are chemically bonded directly to the nickel dopant. These selenium atoms collectively contribute approximately $0.85 \mu_B$, highlighting the strong p-d hybridization between Se p orbitals and Ni d orbitals plays a crucial role in mediating and amplifying the magnetic characteristics of the ZnSe:Ni system. This orbital interaction not only facilitates magnetic exchange coupling but also significantly contributes to the stabilization of the observed ferromagnetic ground state in the material.

Figure 10 represents the spin-polarized density of states (DOS) for the four selenium (Se) atoms chemically bonded to a nickel (Ni) atom in the ZnSe:Ni supercell. The asymmetry between the spin-up and spin-down states near the Fermi level (ϵ_F) indicates a significant spin polarization, suggesting a contribution of these Se atoms to the overall magnetic behavior of the system.

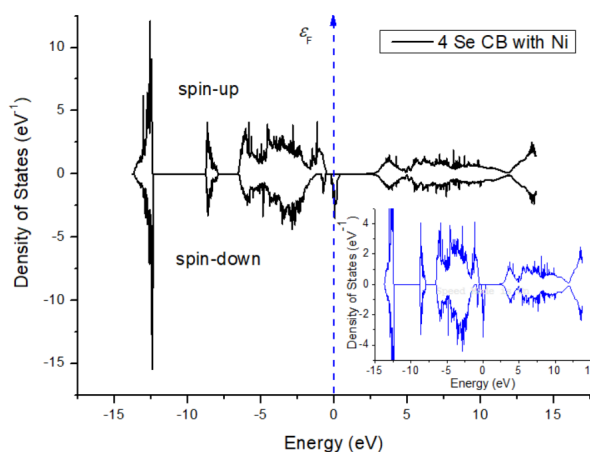


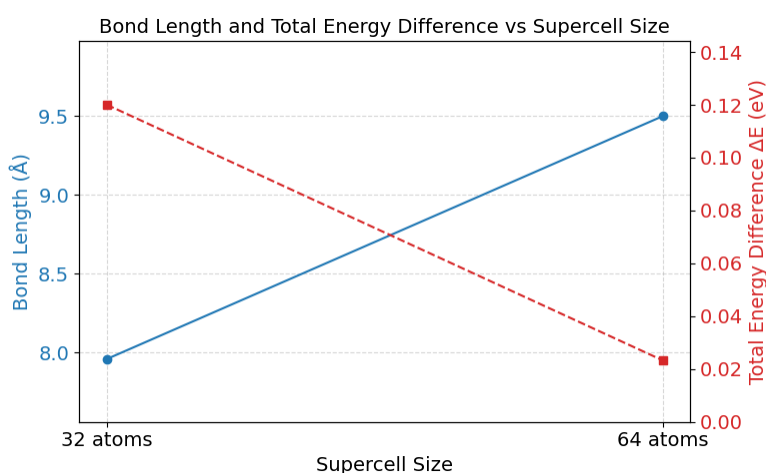
Figure 10. Spin-polarized DOS diagrams of the four selenium atoms chemically bonded to Ni in the ZnSe:Ni supercell structure, illustrating their contribution to the magnetic behavior.

Table 2. Bond lengths between two nickel dopants and total energy differences for Ni-doped ZnSe at 12.5% and 6.25% concentrations

Supercells	Number of atoms	Bond length (Ni-Ni), Å	ΔE [eV]
Zn ₁₄ Ni ₂ Se ₁₆ (2 Ni(Zn)-doped in ZnSe)	32	7.96	0.12004
Zn ₃₀ Ni ₂ Se ₃₂ (2 Ni(Zn)-doped in ZnSe)	64	9.50	0.02328

The theoretically calculated bond distances between two impurity atoms and the energy differences ($\Delta E = E_{\text{AFM}} - E_{\text{FM}}$) for ZnSe:Ni compounds at 12.5 and 6.25 % concentrations are represented in the following Table 2. The total energy difference between the antiferromagnetic (AFM) and ferromagnetic (FM) configurations serves as a critical parameter for evaluating the magnetic stability of Ni-doped ZnSe systems. A positive value of ΔE indicates that the ferromagnetic phase is energetically preferred over the antiferromagnetic one, suggesting a stable ferromagnetic ground state. In our results, the smaller supercell (32 atoms) with a bond length of 7.96 Å shows a larger ΔE (0.12004 eV), indicating stronger ferromagnetic coupling and greater magnetic stability at this doping concentration. Meanwhile, the larger supercell (64 atoms) with a longer bond length of 9.50 Å exhibits a smaller ΔE (0.02328 eV), suggesting weaker ferromagnetic interactions and relatively reduced stability. These findings imply that the magnetic properties and stability of Ni-doped ZnSe are strongly dependent on dopant concentration and spatial arrangement, which is crucial for designing spintronic devices with optimized performance.

Figure 11 describes the variation of total energy difference (ΔE) and bond length (Å) for the different Ni-ZnSe supercell structures containing 32- and 64-atoms. We obtained that increasing the size of the supercell from 32 to 64 atoms results in a noticeable increase in the bond length between two Ni dopants, from 7.96 Å to 9.50 Å. At the same time, the total energy difference decreases from 0.12004 to 0.02328 eV indicates the FM state becomes energetically more favorable in larger supercells, reflecting enhanced magnetic stability with reduced Ni-Ni interaction strength due to increased spatial separation. These results support the idea that dilute Ni doping in ZnSe maintains ferromagnetic stability, particularly at lower concentrations where dopants are more isolated.

**Figure 11.** The variation of total energy difference (ΔE) and bond length (Å) for Ni-ZnSe systems.

Our first-principles results (see Table 2) demonstrate that the FM phase is more stable than the AFM phase in Ni-ZnSe compounds. The spin-polarized band structures and electronic DOS results reveal that nickel doping induces a high-spin state with half-metallic characteristics in the ZnSe supercells. These characteristics underscore the significant promise of Ni-ZnSe as a functional material for advanced technologies, especially in the realm of spintronics, where high spin polarization and robust magnetic stability are critical for device performance.

4. CONCLUSION

In this work, spin-polarized first-principles simulations based on DFT were conducted to explore the magnetic and electronic properties of ZnSe doped by Ni at doping concentrations of 12.5% and 6.25%. The *ab initio* results suggest that the incorporation of nickel substantially modifies the host material's electronic and magnetic structure, giving rise to a half-metallic ferromagnetic state, a feature highly desirable for spintronic applications. The obtained value of magnetic moment of the doped supercells is approximately 4.0 μ_B , where the dominant contribution arises from the localized 3d states of the Ni²⁺ ions, with additional hybridization from the p-states of neighboring Se atoms.

The spin-resolved band structure and DOS analyses confirm the presence of spin polarization near the Fermi energy, indicating potential applicability in spintronic technologies. Furthermore, Mulliken population analysis and spin-density visualizations reveal strong magnetic ordering primarily around Ni sites.

We also evaluated the total energy differences between ferromagnetic (FM) and antiferromagnetic (AFM) configurations. The results consistently show that the FM phase is energetically more favorable, especially at lower

doping concentrations, signifying magnetic stability in diluted Ni configurations. Increasing the size of the supercell results in reduced magnetic interaction between Ni dopants, as reflected by the increased bond length and decreased ΔE values.

Overall, the findings indicate that Ni-ZnSe systems exhibit the key characteristics of a promising DMS materials with half-metallic behavior, positioning it as a strong contender for future applications in spintronic technologies, optoelectronic systems, and magneto-electronic devices.

ORCID

✉ V.N. Jafarova, <https://orcid.org/0000-0002-0643-1464>; ✉ A.N. Jafarova, <https://orcid.org/0000-0001-8150-1787>

✉ A.J. Ahmadova, <https://orcid.org/0009-0004-9657-5649>

REFERENCES

- [1] L. Liu, *et al.*: “Oxygen vacancies: the origin of n-type conductivity in ZnO,” *Physical Review B*, **93**, 235305 (2016). <https://doi.org/10.1103/PhysRevB.93.235305>
- [2] E. A. Zhukov, *et al.*: “Spin coherence of electrons and holes in ZnSe-based quantum wells studied by pump-probe Kerr rotation,” *Physica Status Solidi B*, **251**(9), 1872-1880 (2014). <https://doi.org/10.1002/pssb.201350233>
- [3] L. Ławniczak-Jabłońska, *et al.*: “Correlation between XANES of the transition metals in ZnS and ZnSe and their limit of solubility,” *Physica B: Condensed Matter*, **208**, 497-502 (1995). [https://doi.org/10.1016/0921-4526\(94\)00732-B](https://doi.org/10.1016/0921-4526(94)00732-B)
- [4] D. Theis, “Electronic structure of ZnSe,” *Physica Status Solidi (b)*, **79**, 125 (1977). <https://doi.org/10.1002/pssb.2220790112>
- [5] G. P. Yablonskii, *et al.*: “Optically-Pumped Lasing of Doped ZnSe Epitaxial Layers Grown by Metal-Organic Vapour-Phase Epitaxy,” *Physica Status Solidi (a)* **159**, 543-557 (1997). [https://doi.org/10.1002/1521-396X\(199702\)159:2%3C543::AID-PSSA543%3E3.0.CO;2-S](https://doi.org/10.1002/1521-396X(199702)159:2%3C543::AID-PSSA543%3E3.0.CO;2-S)
- [6] W. Y. Liang and A. D. Yoffe: “Electronic structure of II–VI compounds,” *Proceedings of the Royal Society of London. Series A, Mathematical and Physical Sciences*, **300**, 326 (1967).
- [7] B. Pejova, “The higher excited electronic states and spin-orbit splitting of the valence band in three-dimensional assemblies of close-packed ZnSe and CdSe quantum dots in thin film form,” *Journal of Solid State Chemistry*, **181**(8), 2041-2048 (2008). <https://doi.org/10.1016/j.jssc.2008.03.038>
- [8] T. Dietl, H. Ohno, and F. Matsukura, “Hole-mediated ferromagnetism in tetrahedrally coordinated semiconductors,” *Physical Review B*, **63**, 195205 (2001). <https://doi.org/10.1103/PhysRevB.63.195205>
- [9] M. Tanaka and Y. Higo, “Large tunneling magnetoresistance in GaMnAs/AlAs/GaMnAs ferromagnetic semiconductor tunnel junctions,” *Physical Review Letters*, **87**(2), 026602 (2001). <https://doi.org/10.1103/PhysRevLett.87.026602>
- [10] S. A. Wolf, *et al.*: “Spintronics: A spin-based electronics vision for the future,” *Science*, **294**(5546), 1488-1495 (2001). <https://doi.org/10.1126/science.1065389>
- [11] D. D. Awschalom and M. E. Flatté, “Challenges for semiconductor spintronics,” *Nature Physics*, **3**(3), 153-159 (2007). <https://doi.org/10.1038/nphys551>
- [12] K. Sato, *et al.*: “First-principles theory of dilute magnetic semiconductors,” *Reviews of Modern Physics*, **82**(2), 1633-1690 (2010). <https://doi.org/10.1103/RevModPhys.82.1633>
- [13] F. Goumrhar, *et al.*: “Ab-initio calculations for the magnetic properties of TM(Ti,V)-doped zinc-blende ZnO,” *International Journal of Modern Physics B*, **32**, 1850025 (2018). <https://doi.org/10.1142/S021797921850025X>
- [14] B. Xiao, *et al.*: “Optical and electrical properties of vanadium-doped ZnTe crystals grown by the temperature gradient solution method,” *Optical Materials Express*, **8**, 431-439 (2018). <https://doi.org/10.1364/OME.8.000431>
- [15] W. Benstaali, *et al.*: “Ab-initio study of magnetic, electronic and optical properties of ZnSe doped-transition metals,” *Materials Science in Semiconductor Processing*, **16**, 231 (2013). <http://dx.doi.org/10.1016/j.mssp.2012.10.001>
- [16] C. Kim, *et al.*: “Middle-infrared random lasing of Cr²⁺ doped ZnSe, ZnS, CdSe powders, powders imbedded in polymer liquid solutions, and polymer films,” *Optics Communications*, **282**, 2049-2052 (2009). <https://doi.org/10.1016/j.optcom.2009.02.023>
- [17] J.E. Williams, *et al.*: “Mid-IR laser oscillation in Cr²⁺:ZnSe planar waveguide,” *Optics Express*, **18**, 25999-26006 (2010). <https://doi.org/10.1364/OE.18.025999>
- [18] N. Myoung, *et al.*: “Energy scaling of 4.3 μm room temperature Fe: ZnSe laser,” *Optics Letters* **36**, 94-96 (2011). <https://doi.org/10.1364/OL.36.000094>
- [19] I.S. Moskalev, V.V. Fedorov, S.B. Mirov, “10-Watt, pure continuous-wave, polycrystalline Cr²⁺:ZnS laser,” *Optics Express*, **17**, 2048-2056 (2009). <https://doi.org/10.1364/oe.17.002048>
- [20] V.I. Kozlovsky, *et al.*: “Room-temperature tunable mid-infrared lasers on transition-metal doped II–VI compound crystals grown from vapor phase,” *Physica Status Solidi B*, **247**, 1553-1556 (2010). <http://dx.doi.org/10.1002/pssb.200983165>
- [21] S.ZH. Karazanov, *et al.*: “Electronic structure and optical properties of ZnX (X=O, S, Se, Te): A density functional study,” *Physical Review B*, **75**, 155104 (2007). <http://dx.doi.org/10.1103/PhysRevB.75.155104>
- [22] K. Sato, and H. Katayama-Yoshida, “Ab initio Study on the Magnetism in ZnO-, ZnS-, ZnSe and ZnTe-Based Diluted Magnetic Semiconductors,” *Physica Status Solidi (b)*, **229**, 673-680 (2002). [https://doi.org/10.1002/1521-3951\(200201\)229:2%3C673::AID-PSSB673%3E3.0.CO;2-7](https://doi.org/10.1002/1521-3951(200201)229:2%3C673::AID-PSSB673%3E3.0.CO;2-7)
- [23] Q. Mahmood, *et al.*: “The study of electronic, elastic, magnetic and optical response of Zn_{1-x}Ti_xY (Y = S, Se) through mBJ potential,” *Current Applied Physics*, **16**, 549-561 (2016). <https://doi.org/10.1016/j.cap.2016.03.002>
- [24] S. Arif, *et al.*: “Investigation of half metallicity in Fe doped CdSe and Co doped CdSe materials,” *Current Applied Physics*, **12**, 184-187 (2012). <https://doi.org/10.1016/j.cap.2011.05.034>
- [25] V.N. Jafarova, “Study the electronic and magnetic properties of Mn-doped wurtzite ZnSe using first-principle calculations,” *Indian Journal of Physics*, **97**, 2639-2647 (2023). <http://dx.doi.org/10.1007/s12648-023-02598-y>
- [26] P. Hohenberg, and W. Khon, “Inhomogeneous electron gas,” *Physical Review B*, **136**, 864-871 (1964). <https://doi.org/10.1103/PhysRev.136.B864>

- [27] D.M. Ceperley, and B.J. Alder, "Ground state of the electron gas by a stochastic method," *Physical Review Letters*, **45**, 566-569 (1980). <https://doi.org/10.1103/PhysRevLett.45.566>
- [28] M. Cococcioni, and S. De Gironcoli, "Linear response approach to the calculation of the effective interaction parameters in the LDA+U method," *Physical Review B*, **71**, 035105 (2005). <https://doi.org/10.1103/PhysRevB.71.035105>
- [29] V.N. Jafarova, "Ab-initio calculation of structural and electronic properties of ZnO and ZnSe compounds with wurtzite structure," *International Journal of Modern Physics B*, **36**, 2250156 (2022). <https://doi.org/10.1142/S0217979222501569>
- [30] V.N. Jafarova, and M.A. Musaev, "First-principles study of structural and electronic properties of ZnSe with wurtzite structure," *Technium: Romanian Journal of Applied Sciences and Technology*, **6**, 42-46 (2023).
- [31] R.W.G. Wyckoff, *Crystal Structures*, Second Edition, (Interscience Publishers, New York, 1963). <https://search.worldcat.org/search?q=au=%22Wyckoff%2C%20R.%20W.%20G.%22>
- [32] V.N. Jafarova, and H.S. Orudzhev, "Structural and electronic properties of ZnO: A first-principles density-functional theory study within LDA(GGA) and LDA(GGA)+ U methods," *Solid State Communications*, **325**, 114166 (2021). <https://doi.org/10.1016/j.ssc.2020.114166>
- [33] R. D. Shannon, "Revised effective ionic radii and systematic studies of interatomic distances in halides and chalcogenides," *Acta Crystallographica Section A*, **32**(5), 751-767 (1976). <https://doi.org/10.1107/S0567739476001551>

СПІН-ПОЛЯРИЗОВАНІ ВЛАСТИВОСТІ ZnSe, ЛЕГОВАНОГО Ni: МОДЕЛЮВАННЯ ТА СИМУЛЯЦІЇ НА ОСНОВІ ПЕРШИХ ПРИНЦИПІВ

В.Н. Джафарова^{a,b}, А.Н. Джафарова^a, А.Дж. Ахмадова^c

^aАзербайджанський державний університет нафти та промисловості, 20 Azalig Ave., AZ-1010, Баку, Азербайджан

^bХазарський університет, 41 Mehseti Str., AZ1096, Баку, Азербайджан

^cДержавний університет Нахчівана, AZ 7012 Нахчіван, Азербайджан

У цьому дослідженні проведено всебічний *ab initio* аналіз електронних та магнітних властивостей систем ZnSe, легованих нікелем, досліджених при трьох концентраціях домішок – 3,125 %, 6,25% та 12,5%. Аналіз виконано за допомогою теорії функціонала густини (DFT) у рамках локального наближення спінової густини (LSDA), доповненого корекціями Габбарда U для точного врахування сильних ефектів електронної кореляції, характерних для d-орбіталей перехідних металів. Введення атомів Ni в решітку ZnSe суттєво змінює електронну структуру, викликаючи напівметалічну поведінку та виражену спінову поляризацію. Загальний магнітний момент становить приблизно 4,0 мв на суперкомірку. Крім того, порівняння енергій ферромагнітного та антиферромагнітного станів показало, що ферромагнітна фаза є більш стабільною з енергетичної точки зору. Ці результати підкреслюють потенціал ZnSe, легованого Ni, для застосування у спінтроніці, де критично важливим є точний контроль магнітних та електронних властивостей.

Ключові слова: ZnSe:Ni; ферромагнетик; напівметал; магнітний момент; моделювання на основі першопринципів; теорія функціонала густини